



A Computational Approach for Stent Elution Rate Determined Specific Drug Binding and Receptor-mediated Effects in Arterial Tissue

Ramprosad Saha*

Department of Mathematics, Suri Vidyasagar College (Affiliated by University of Burdwan), Suri - 731101, West Bengal, India

Abstract

Background and objective: In the present article the effects of drug binding (both specific and nonspecific) in the porous arterial wall following stent-based drug delivery from drug-eluting stents (DES^s) are investigated. A three-phase (free, extracellular matrix-bound, and specific receptor-bound) second-order nonlinear saturable reversible binding model is considered in order to describe the binding process with the constituents of the porous arterial wall. Although, there are currently some precise forms of a drug binding model in the arterial tissue in the literature, analyzed by various authors. The specific interest in this present context is in assessing to what extent modelling of specific and nonspecific binding within a single-layered homogeneous porous arterial wall is possible. A novel axi-symmetric model of drug delivery from three stent struts has been developed and is presented.

Methods: The governing equations of motion together with the physiologically realistic boundary conditions are tackled numerically by an explicit finite-difference scheme in staggered grids.

Results: Results include the influence of the significant model parameters, such as Peclet numbers (Pe_T , Pe_1 and Pe_2), Damköhler numbers (Da_1 and Da_2) and time-dependent release kinetics as well as constant release kinetics. Consistency of the proposed approach is shown graphically.

Conclusions: As the porosity (ϵ_w) increases, the effective as well as the true diffusivity increases, which eventually leads to expedition of the diffusion process. In a porous media, diffusion takes place in confined tortuous pores and its progression is impeded as the tortuosity increases. The present simulation also demonstrates a decrease in the mean concentration of free as well as extracellular matrix-bound and SR-bound drug with increasing tortuosity. The present observation may be justified in the sense that as the tortuosity increases so too does the effective distance over which diffusion has to take place (*i.e.* the progression of diffusion is impeded, which eventually lowers the mean concentration of all drug forms).

Introduction

Arterial stents are medical devices that have revolutionized the

treatment of coronary artery disease. They serve to reopen the occluded vessel that has become narrowed as a result of atherosclerosis. Atherosclerosis is a common degenerative disease that affects coronary, carotid and other peripheral arteries in the body. Now, it is standard to use the types of stents that gradually release anti-proliferative/anti-inflammatory drugs into the arterial wall to inhibit the cell proliferation that causes the development of restenosis (re-narrowing). The bare metal stents (BMS^s), while revolutionary at the time, were soon rendered unsatisfactory due to their inability to prevent in-stent restenosis. The next wave of drug-eluting stents (DES^s) consists of a supporting metallic wired scaffold coated with a polymer film that encapsulates the therapeutic drug aimed at preventing hyperplasia of the smooth muscle cells (SMC^s) that is responsible for restenosis.

In order to control the release rate, the coating may include a rate-limiting barrier. To ensure effective performance of DES, both

Keywords: Drug-eluting stent; Free drug; ECM-bound drug; SR-bound drug; Convection-diffusion-reaction; Peclet number; Damköhler number.

Abbreviations: 2D, two-dimensional; BMS, bare metal stents; DES, drug-eluting stents; ECM, extracellular matrix; MAC, marker and cell; PCI, percutaneous coronary interventions; SDR, specific drug binding; SER, stent elution rate; SMC, smooth muscle cells; SR, specific receptors.

Received: July 12, 2018; Revised: November 25, 2018; Accepted: November 27, 2018

*Correspondence to: Ramprosad Saha, Department of Mathematics, Suri Vidyasagar College (Affiliated by University of Burdwan), Suri - 731101, West Bengal, India. Tel/Fax: +91-3462-255504; E-mail: itsramprasadh@gmail.com

How to cite this article: Saha R. A Computational Approach for Stent Elution Rate Determined Specific Drug Binding and Receptor-mediated Effects in Arterial Tissue. *J Explor Res Pharmacol* 2018;3(4):105–118. doi: 10.14218/JERP.2018.00018.

the stent geometry and coating design need to be optimized so that therapeutic levels of drug are delivered to the arterial wall for the required period of time.^{1,2} The success of an anti-proliferative drug therapy from DES depends on the amount of drug eluted from the stent, accumulation of the drug, and drug binding to cells in the arterial wall. Even though DES are now the primary choice of percutaneous coronary interventions (PCI^s) for millions of patients, many questions still remain unanswered regarding their longevity and safety.

Although it was not the intention of this article to provide a review of the previously published models, it will describe some experimental studies which have been carried out in the recent past in order to quantify the capability of this device to reduce the in-stent restenosis rate after stent implantation.³⁻⁵ The behavior of heparin in explanted arteries allows for the presence of binding site changes along the transmural direction, being higher in the endothelium and lower in the adventitia, as studied by Lovich *et al.*³ In the experimental study by Migliavacca *et al.*,⁶ the pattern of DES drug release in the vascular wall was considered using a single species approach along with a partition coefficient approach to relate the free and the bound drug concentrations. Borgi *et al.*⁷ focused on the inclusion of reversible binding leading to delayed release and that the erosion of polymer affects the drug release from a single strut. Horner *et al.*⁸ appear to be one of the first groups to provide a three-dimensional reaction-diffusion-convection process of a two-species drug delivery model, including reversible binding sites in a realistic geometry; their model predicted that a single species drug delivery model cannot accurately predict the distribution of the bound drug. Ferreira *et al.*⁹ considered a series of nonlinear binding models to describe the degradation of a poly-L-lactic acid stent coating into lactic acid and oligomers.

Although a large number of mathematical models are available to describe drug transport and its binding to arterial tissue sites, only a few (*v.i.z.* Tzafiriri *et al.*¹⁰) considered a nonlinear saturable binding model; later, Bozsak *et al.*^{11,12} also considered this. The model from the latter included two phases of drug in the tissue: free and bound. However, it is well established that in addition to binding to specific receptors (SR), there is also the occurrence of nonspecific binding caused by association of drug with membrane constituents or by trapping of the drug in the extracellular medium.¹³ Most recently, Tzafiriri *et al.*¹⁴ and McGinty *et al.*¹⁵ included two equations for drug binding in arterial tissue, namely one for specific binding to receptors and another for nonspecific binding to general extracellular matrix (ECM) sites. Thus, it appears that there are three phases in the tissue, comprising two bound (SR and ECM) and one free.

The main aim of this investigation was to extend the aforementioned work^{14,15} with a two-species model of specific and nonspecific saturable binding in the arterial wall at different phases following drug transport eluted from three struts, where the transport of free drug is governed by a convection-diffusion-reaction process and that of bound drugs (SR and ECM) by a reaction process only. A simple time-dependent release kinetics is implemented on the surface of the struts.¹⁶ The transport of drugs within the arterial tissue is controlled by arterial properties like porosity and tortuosity. At the time of implantation of an endovascular DES, its major impact is on the structure of the arterial wall, which eventually influences the overall rates of diffusion through tissues. The effective diffusivity of a porous wall is supposed to depend on two factors, such as porosity and tortuosity—these parameters regulate the free diffusivity of the drug eluted from struts.¹⁷ As such, the present study also deals with the effects of porosity and tortuosity on the diffusivity of

Table 1. Nomenclature

Nomenclature	
L	Dimensionless length of the artery
C_s	Initial drug concentration on the stent
V_{wall}	Transmural filtration velocity
\bar{r}	Dimensional radial coordinate
r	Dimensionless radial coordinate
\bar{z}	Dimensional axial coordinate
z	Dimensionless axial coordinate
\bar{t}	Dimensional time
t	Dimensionless time
\bar{C}_f	Dimensional concentration of free drug
C_f	Dimensionless concentration of free drug
\bar{C}_{ECM}	Dimensional concentration of ECM-bound drug
C_{ECM}	Dimensionless concentration of ECM-bound drug
\bar{C}_{DSR}	Dimensional concentration of SR-bound drug
C_{DSR}	Dimensionless concentration of SR-bound drug
C_{ECM}^{max}	ECM binding site density
C_{DSR}^{max}	Receptor density
B_M	Total tissue binding capacity
K_d^{ECM}	ECM binding on-rate
k_{on}^{SR}	Receptor binding on-rate
K_d	Equilibrium association constant
K_d^{ECM}	ECM dissociation constant
K_d^{SR}	Receptor dissociation constant
D_{free}	Free drug diffusivity
D_{eff}	Effective diffusivity of free drug
D_T	True drug diffusivity of arterial wall
D_T^{ECM}	True drug diffusivity of ECM sites
D_T^{SR}	True drug diffusivity of SR sites
Pe_T	Non-dimensional Peclet number
Pe_1	Non-dimensional Peclet number
Pe_2	Non-dimensional Peclet number
Da_1	Dimensionless Damköhler number
Da_2	Dimensionless Damköhler number
Greek Symbols	
δ	Strut height
α	Non-dimensional parameter
α_1	Non-dimensional parameter
β	Non-dimensional parameter
β_1	Non-dimensional parameter
ϵ_w	Porosity of the arterial wall

Table 1. Nomenclature - (continued)

Greek Symbols	
γ_w	Hindrance coefficient of arterial wall
τ_w	Tortuosity of the arterial wall
λ	Dimensional drug release rate
λ	Dimensionless drug release rate
r_{ti}	Proximal wall
r_{to}	Distal wall
r_{tl}	Arterial lower wall
r_{tp}	Perivascular wall
r_{bt}	Lumen-tissue interface
r_{st}	Strut-tissue interface
Subscripts	
f	Free
b	Bound
ECM	Extra cellular matrix
SR	Receptor

drug.

Materials and methods

Please refer to Table 1 for nomenclature.

Geometric model

The computational domain is comprised of a long axial section of length L and the wall thickness is taken to be 10 times the strut height (δ). The axis of symmetry is taken along the centerline of the artery (cf. Fig. 1). The volume-averaged molar concentra-

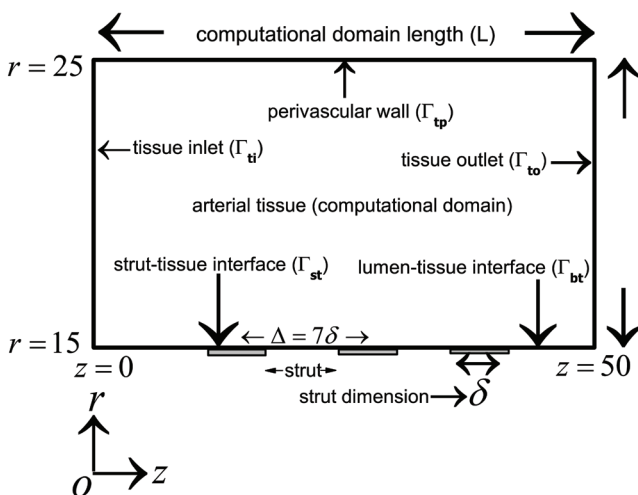


Fig. 1. Schematic of the computational model used for the study.

tion of free drug is denoted by \bar{c}_f the volume-averaged molar concentration of bound drug that is bound to nonspecific general ECM sites in the tissue is referred to as ECM-bound drug and denoted by \bar{c}_{bECM} and the volume-averaged molar concentration of bound drug that is bound to specific receptors is referred to as SR-bound drug and denoted by \bar{c}_{bSR} . The inter-conversion of drug between the unbound plasma phase and the bound phase of tissue binding sites is controlled by a second-order nonlinear reversible saturable chemical reaction. The transport of free drug eluted from struts is governed by unsteady convection-diffusion-reaction process (Eq. 1),¹⁸⁻²⁰ the ECM-bound drug is represented by unsteady reaction process (Eq. 2),²¹ and that of the SR-bound drug is represented by unsteady reaction process (Eq. 3).²² Symmetry boundary conditions for both the free and both of the bound drugs are applied at the proximal (r_{ti}) and the distal (r_{to}) walls (Eq. 4).²³ Impermeable boundary condition for both of the bound drugs is assumed at the perivascular wall (r_{tp}), lumen-tissue (r_{bt}) and strut-tissue (r_{st}) interfaces (Eq. 5). For the free drug, a perfectly sink condition is imposed at the perivascular end (Eq. 6). Since a proper boundary condition for the free drug at lumen-tissue interface (r_{bt}) is not readily apparent, two opposing extremes consider either that flowing blood is extremely efficient at washing out mural-adhered drug, modelled as a zero-concentration interface condition, or mural-adhered drug is insensitive to flowing blood, modelled as a zero-flux boundary condition (Eq. 7).²⁴ Instead of modelling a uniform release of drug from struts, a simple time-dependent release kinetics (Eq. 8)^{25,26} is assumed.

Governing equations and boundary conditions

Therefore, the governing equations of the drug transport of free, ECM-bound (saturable binding to general ECM sites) and SR-bound (saturable binding to specific receptors) in the arterial wall are respectively represented in a two-dimensional (2D) Cartesian coordinate system in the following manner:

$$\frac{\partial \bar{c}_f}{\partial \bar{t}} + \frac{\gamma_w}{\epsilon_w} \frac{\partial (V_{wall} \bar{c}_f)}{\partial \bar{r}} = D_T \left[\frac{\partial^2 \bar{c}_f}{\partial \bar{r}^2} + \frac{1}{\bar{r}} \frac{\partial \bar{c}_f}{\partial \bar{r}} + \frac{\partial^2 \bar{c}_f}{\partial \bar{z}^2} \right] - \frac{\partial \bar{c}_{bECM}}{\partial \bar{t}} - \frac{\partial \bar{c}_{bSR}}{\partial \bar{t}}, \tag{1}$$

$$\frac{\partial \bar{c}_{bECM}}{\partial \bar{t}} = \left[k_{on}^{ECM} \bar{c}_f (\bar{c}_{bECM}^{max} - \bar{c}_{bECM}) - k_{on}^{ECM} K_d^{ECM} \bar{c}_{bECM} \right], \tag{2}$$

$$\frac{\partial \bar{c}_{bSR}}{\partial \bar{t}} = \left[k_{on}^{SR} \bar{c}_f (\bar{c}_{bSR}^{max} - \bar{c}_{bSR}) - k_{on}^{SR} K_d^{SR} \bar{c}_{bSR} \right], \tag{3}$$

Where \bar{t} denotes time since stent implantation, \bar{r} is the distance from the intima, \bar{c}_f is the molar concentration of free drug per unit tissue volume, \bar{c}_{bECM} and \bar{c}_{bSR} are the molar concentrations of ECM- and receptor-bound drug respectively, \bar{c}_{bECM}^{max} and \bar{c}_{bSR}^{max} denote the local molar concentration of ECM and receptor drug binding sites respectively, k_{on}^{ECM} and k_{on}^{SR} are the respective binding on-rate constants, K_d^{ECM} and K_d^{SR} are the respective equilibrium dissociation constants, and V_{wall} is its transmural convective velocity. Here, D_T is the transmural true diffusivity of the drug which can be written

as 17.27

$$D_T = [1 + \frac{B_M}{K_d}] \times D_{eff}$$

where

$$D_{eff} = \frac{\epsilon_w}{\tau_w} \times D_{free}$$

Here, ϵ_w and τ_w are the porosity and the tortuosity of the wall material respectively, D_{free} and D_{eff} are the coefficients of free and effective diffusivity respectively, B_M and K_d are the net tissue binding capacity and equilibrium association constant respectively.

The symmetry boundary conditions (free, ECM-bound and SR-bound drug) are imposed on the proximal (Γ_{ti}) and the distal (Γ_{to}) walls as

$$\frac{\partial \bar{c}_f}{\partial z} = 0 = \frac{\partial \bar{c}_{b_{ECM}}}{\partial z} = \frac{\partial \bar{c}_{b_{SR}}}{\partial z} \text{ on } \Gamma_{ti} \text{ and } \Gamma_{to}, \quad (4)$$

The impermeable boundary condition for both of the bound drugs (ECM-bound and SR-bound) is assumed at the perivascular wall (Γ_{ip}), lumen-tissue (Γ_{bt}) and strut-tissue (Γ_{st}) interfaces as

$$\frac{\partial \bar{c}_{b_{ECM}}}{\partial r} = 0 = \frac{\partial \bar{c}_{b_{SR}}}{\partial r} \text{ on } \Gamma_{tl} (= \Gamma_{bt} \cup \Gamma_{st}) \text{ and } \Gamma_{ip}, \quad (5)$$

At the perivascular wall (Γ_{ip}), a perfectly sink condition^{4,11} is imposed for the free drug (\bar{c}_f) as

$$\bar{c}_f = 0 \text{ on } \Gamma_{ip}, \quad (6)$$

At the lumen-tissue interface (Γ_{bt}) a proper boundary condition for the free drug is not readily apparent. Considering two opposing extremes, either the flowing blood is extremely efficient at washing out mural-adhered drug, modelled as a zero-concentration interface condition, or mural-adhered drug is insensitive to flowing blood, modelled as zero-flux boundary condition as

$$\bar{c}_f = 0 \text{ or } \frac{\partial \bar{c}_f}{\partial r} = 0 \text{ on } \Gamma_{bt}, \quad (7)$$

As the dimension of stent struts is thin with respect to the arterial wall thickness, so their actual geometry is neglected and approximate the drug eluting stent using an equivalent phantom surface that elutes a defined drug load to the arterial wall (Fig. 1). Elution from the phantom surface is modelled by a simple time-dependent release kinetics as follows

$$\bar{c}_f = c_s \exp(-\bar{\lambda} \bar{t}); \bar{t} \geq 0 \text{ on } \Gamma_{st}, \quad (8)$$

where c_s is the initial drug concentration on the stent, and $\bar{\lambda}$ is the stent drug decay rate.

All the variables and parameters are now made dimensionless to obtain well-behaved computations in the following manner:

$$r = \frac{\bar{r}}{\delta}, z = \frac{\bar{z}}{\delta}, t = \frac{\bar{t} \cdot V_{wall}}{\delta},$$

$$c_f = \frac{\bar{c}_f}{c_s}, c_{b_{ECM}} = \frac{\bar{c}_{b_{ECM}}}{c_{b_{ECM}}^{max}}, c_{b_{SR}} = \frac{\bar{c}_{b_{SR}}}{c_{b_{SR}}^{max}}$$

Under these assumptions, the above equations (1–8) take their respective non-dimensional forms as follows:

$$\frac{\partial c_f}{\partial t} + \frac{\gamma_w}{\epsilon_w} \frac{\partial c_f}{\partial r} = \frac{1}{Pe_T} \left[\frac{\partial^2 c_f}{\partial r^2} + \frac{1}{r} \frac{\partial c_f}{\partial r} + \frac{\partial^2 c_f}{\partial z^2} \right] - \frac{1}{\alpha} \frac{\partial c_{b_{ECM}}}{\partial t} - \frac{1}{\beta} \frac{\partial c_{b_{SR}}}{\partial t}, \quad (9)$$

$$\frac{\partial c_{b_{ECM}}}{\partial t} = \frac{\alpha Da_1}{Pe_1} \left[c_f (1 - c_{b_{ECM}}) - \alpha_1 c_{b_{ECM}} \right], \quad (10)$$

$$\frac{\partial c_{b_{SR}}}{\partial t} = \frac{\beta Da_2}{Pe_2} \left[c_f (1 - c_{b_{SR}}) - \beta_1 c_{b_{SR}} \right], \quad (11)$$

$$\frac{\partial c_f}{\partial z} = 0 = \frac{\partial c_{b_{ECM}}}{\partial z} = \frac{\partial c_{b_{SR}}}{\partial z} \text{ on } \Gamma_{ti} \text{ and } \Gamma_{to}, \quad (12)$$

$$\frac{\partial c_{b_{ECM}}}{\partial r} = 0 = \frac{\partial c_{b_{SR}}}{\partial r} \text{ on } \Gamma_{tl} (= \Gamma_{bt} \cup \Gamma_{st}) \text{ and } \Gamma_{ip}, \quad (13)$$

$$c_f = 0 \text{ on } \Gamma_{ip}, \quad (14)$$

$$c_f = 0 \text{ or } \frac{\partial c_f}{\partial r} = 0 \text{ on } \Gamma_{bt}, \quad (15)$$

$$c_f = c_s \exp(-\lambda t); t \geq 0 \text{ on } \Gamma_{st}, \quad (16)$$

where the Peclet numbers (Pe_T, Pe_1 and Pe_2), the Damköhler numbers (Da_1 and Da_2), the scaling parameters (α, α_1, β and β_1) and dimensionless drug release rate (λ) are defined respectively as:

$$Pe_T = \frac{V_{wall} \cdot \delta}{D_T}, Pe_i = \frac{V_{wall} \cdot \delta}{D_T^{(i)}}, Da_i = \frac{k_{on}^{(i)} \cdot c_{b(i)}^{max} \cdot \delta^2}{D_T^{(i)}} \quad (i = 1, 2; (1) \rightarrow \text{ECM and } (2) \rightarrow \text{SR})$$

$$\alpha = \frac{c_s}{c_{b_{ECM}}^{max}}, \alpha_1 = \frac{K_d^{ECM}}{c_s}, \beta = \frac{c_s}{c_{b_{SR}}^{max}}, \beta_1 = \frac{K_d^{SR}}{c_s}, \lambda = \frac{\bar{\lambda} \cdot \delta}{V_{wall}}$$

where $K_d^{ECM} (k_r^{ECM}/k_{on}^{ECM})$ and $K_d^{SR} (k_r^{SR}/k_{on}^{SR})$ are, respectively, the equilibrium dissociation constants of the ECM-bound drug and the SR-bound drug, k_r^{ECM} and k_r^{SR} are the dissociation (backward) rate constant of ECM and receptor drug binding sites in the arterial tissue respectively. Here, D_T^{ECM} and D_T^{SR} are, respectively, the true diffusivities of the ECM-bound drug and the SR-bound drug.

Solution procedure

The governing equations (9–11) representing the transport of free, ECM-bound and SR-bound drugs were solved numerically using a finite-difference scheme by applying the time-dependent release kinetics and boundary conditions (12–16). For this type of grid

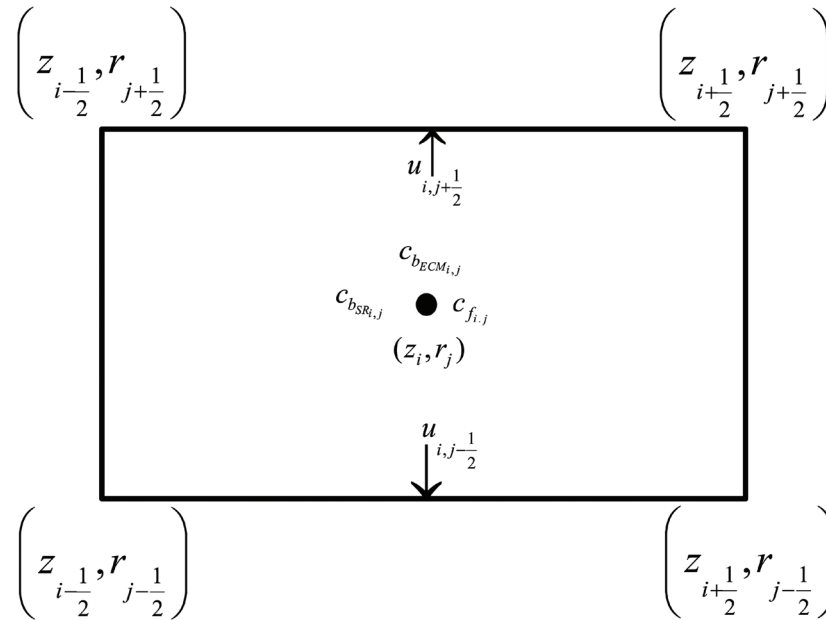


Fig. 2. A typical combined MAC cell for tissue. Abbreviation: MAC, marker and cell.

alignment, the concentrations for free, ECM-bound and SR-bound drugs were calculated at the cell centers (Fig. 2). The discretization of the time derivative term was based on the first order accurate two-level forward time-differencing formula, while the convective term in the equations is accorded with a hybrid formula, consisting of central differencing and second order up-winding. The diffusive terms are, however, discretized by a second order accurate three-point central difference formula. In order to have second order spatial accuracy of the boundary conditions, some fictitious grid points outside the physical domain were considered. To achieve the steady state criterion, one needs to perform at least 8,00,000 iteration steps for the marker and cell (MAC) scheme. Steady state is achieved when the convergence criterion for concentration is 10^{-6} for each drug form. Interested readers are referred to Saha *et al.*²⁸ for the detailed numerical procedure.

Results and discussion

For the purpose of numerical computation of the quantities of physiological significance, the computational domain has been confined to a finite non-dimensional arterial length of 50. For this computational domain, solutions are computed with grid sizes 501×101 for $\delta t = 0.0001$.

Based on the numerical values in Table 2^{10,14,17,19,22,23,27,29-39} of the model parameters, an extensive quantitative analysis has been performed through graphical representations, the results are presented in Figures 3–14. These are representative of a first-generation DES (Cypher) which elutes the drug sirolimus. The radial locations-variant normalized concentration profiles for free drug, ECM-bound drug and SR-bound drug concentrations in the tissue for three different times have been shown in Figure 3a–c respectively. It was observed from the figures that with increasing time, the drug masses (free, ECM-bound and SR-bound) decrease (at $z = 21.5$). The rate of decrease for the free drug is faster than the ECM-bound drug, whereas the SR-bound drug is slower than the ECM-bound drug. As a result, the drug enters the arterial wall (at

$r = 15$) in the free phase and is rapidly bound to both ECM and SR binding sites. The free and ECM-bound drug concentration profiles rise to a peak (shown in Fig. 3d) before decaying with time as the drug traverses through the tissue, becomes bound to SR in the binding phase, and is absorbed at the adventitial boundary ($r = 25$).

Although the free and ECM-bound phase profile shapes are similar, drug concentrations within the SR-bound phase are greater

Table 2. Plausible values of involved parameters

Parameter	Value with unit	Reference
δ	10^{-4} m	[19,29,37]
C_s	10^{-2} mol m ⁻³	[35]
V_{wall}	5.8×10^{-8} m s ⁻¹	[31,36]
C_{ECM}^{max}	3.63×10^{-1} mol m ⁻³	[10]
C_{DSR}^{max}	3.3×10^{-3} mol m ⁻³	[14]
B_M	1.3 mol m ⁻³	[27]
K_{on}^{ECM}	2.0 [mol m ⁻³ s] ⁻¹	[10]
K_{on}^{SR}	8.0×10^2 [mol m ⁻³ s] ⁻¹	[38]
K_d	0.136 mol m ⁻³	[27]
K_d^{ECM}	2.6×10^{-3} mol m ⁻³	[10]
K_d^{SR}	2.0×10^{-5} mol m ⁻³	[22]
k_r^{ECM}	5.2×10^{-3} s ⁻¹	[14]
k_r^{SR}	1.6×10^{-3} s ⁻¹	[14]
D_{free}	3.65×10^{-12} m ² s ⁻¹	[23,32]
$\bar{\lambda}$	10^{-5} s ⁻¹	[33,34]
ϵ_w	0.787	[17]
γ_w	1	[30,39]
τ_w	1.333	[17]

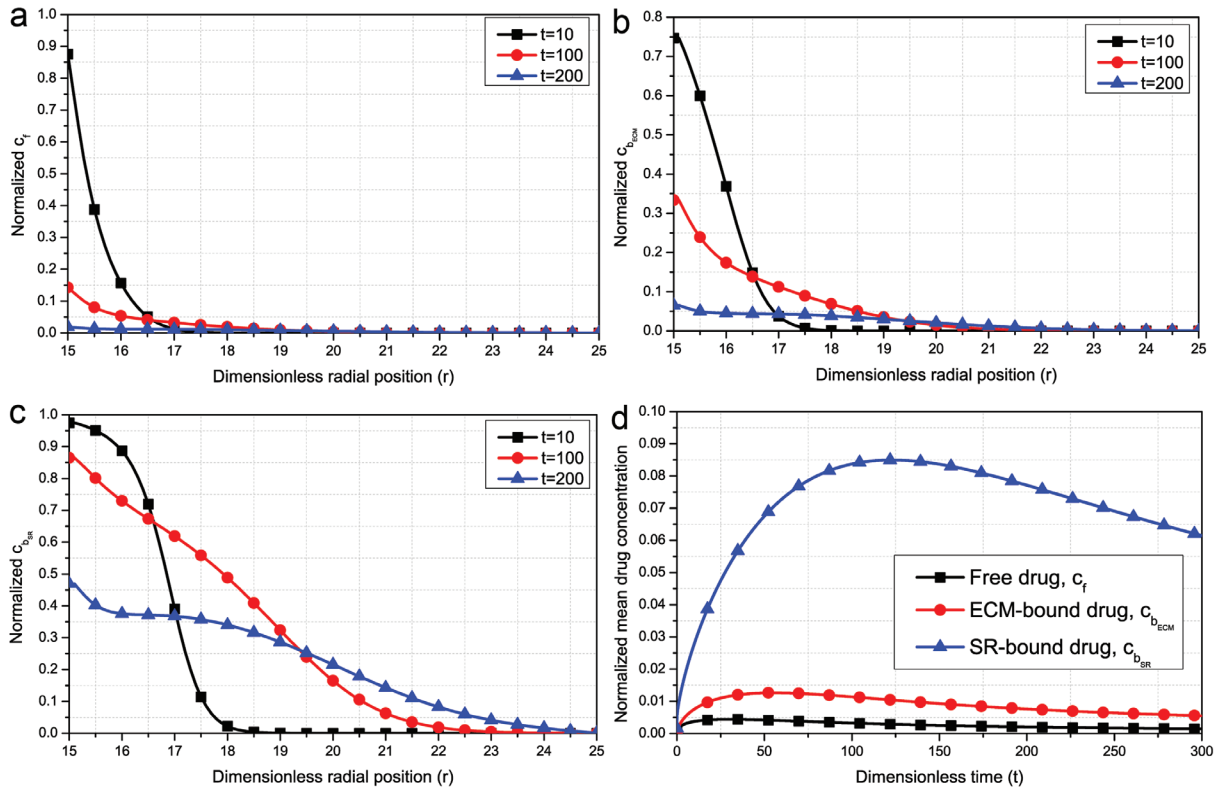


Fig. 3. Drug concentration in the vessel wall versus transmural positions for different times at $z = 21.5$. (a) Free drug; (b) ECM-bound drug; (c) SR-bound drug; (d) Non-dimensional drug mass in each phase versus time. Other model parameters are set as in Table 2. Abbreviations: ECM, extracellular matrix; SR, specific receptors.

than in the ECM-bound phase, which in turn is greater than the free drug concentrations. Within the time $t = 10$, the SR-bound drug spanning 30% the thickness of the tissue is saturated; these remain saturated for the duration of the time $t = 200$ studied (Fig. 3c). The remaining SR sites become saturated in the subsequent times and they too remain at saturation levels for the duration of the times $t = 300$. In Figure 3d, the temporal variation of normalized mean drug concentration profiles reveals that the drug binding in the SR-bound phase is higher than the drug binding in the ECM-bound phase. Therefore, the results of this study demonstrate that drug delivered to the arterial wall from the stent is too low to occupy a large proportion of ECM binding sites, yet is high enough to saturate SR binding sites. This agrees with Tzafirri *et al.*¹⁴

The time-variant concentration profiles for free drug, ECM-bound drug and SR-bound drug concentrations in the tissue for different radial locations are shown in Figure 4a–c respectively. It was observed from these figures that with increasing radial locations (from lumen-tissue interface), the drug masses (free, ECM-bound and SR-bound) decrease (at $z = 21.5$). The characteristics of the graphs are quite similar, as anticipated, with the binding and unbinding processes taking place simultaneously. Moreover, at the interface, it has been observed that the concentration of drug attains its maximum value for all time, as expected.

Distributions of normalized mean free drug, mean ECM-bound drug, mean SR-bound drug and mean total drug concentrations over the entire period of time for different values of the Peclet number Pe_T are presented in Figure 5a–d respectively. It is observed that in each case the drug mass is first increasing, up to some upper bound, and then decreasing asymptotically. Evidently, Pe_T depend-

ing on D_T , again D_T depends on D_{eff} , increases with a decrease of the porosity (ϵ_w) of the arterial wall (as the porosity decreases, the effective as well as true diffusivity does decrease), and also with an increase of the tortuosity (τ_w) of the arterial wall (as the tortuosity increases, the effective diffusivity as well as true diffusivity does decrease) (keeping D_{free} fixed). It is observed from these figures that all the mean drug (free, ECM-bound, SR-bound and total) concentrations decrease with decreasing porosity and increasing tortuosity of the arterial wall (*i.e.* increase of the Peclet number (Pe_T)).

The influence of scaling parameter Da_1/Pe_1 on the normalized mean free drug, mean ECM-bound drug, mean SR-bound drug and mean total drug concentrations in the arterial tissue are displayed in Figure 6a–d respectively over a stipulated period of time. Evidently, Da_1/Pe_1 , depending on k_{on}^{ECM} and c_{DECM}^{max} (keeping δ and V_{wall} fixed), increases/decreases with an increase/decrease in the ECM binding site density (c_{DECM}^{max}) and also with an increase/decrease of ECM binding on-rate (k_{on}^{ECM}). It has been observed that with increasing ECM binding site density and ECM binding on-rate (*i.e.* increase of Da_1/Pe_1), the mean drug (free, SR-bound and total) concentrations decrease. But, the mean ECM-bound drug concentration increases with increasing ECM binding site density and ECM binding on-rate (*i.e.* increase of Da_1/Pe_1).

The influence of scaling parameter Da_2/Pe_2 on the normalized mean free drug, mean ECM-bound drug, mean SR-bound drug and mean total drug concentrations in the arterial tissue are displayed in Figure 7a–d respectively over a stipulated period of time. Evidently, Da_2/Pe_2 , depending on k_{on}^{SR} and c_{DSR}^{max} (keeping δ and V_{wall} fixed), increases/decreases with an increase/decrease in the receptor binding site density (c_{DSR}^{max}) and also with an increase/decrease in receptor

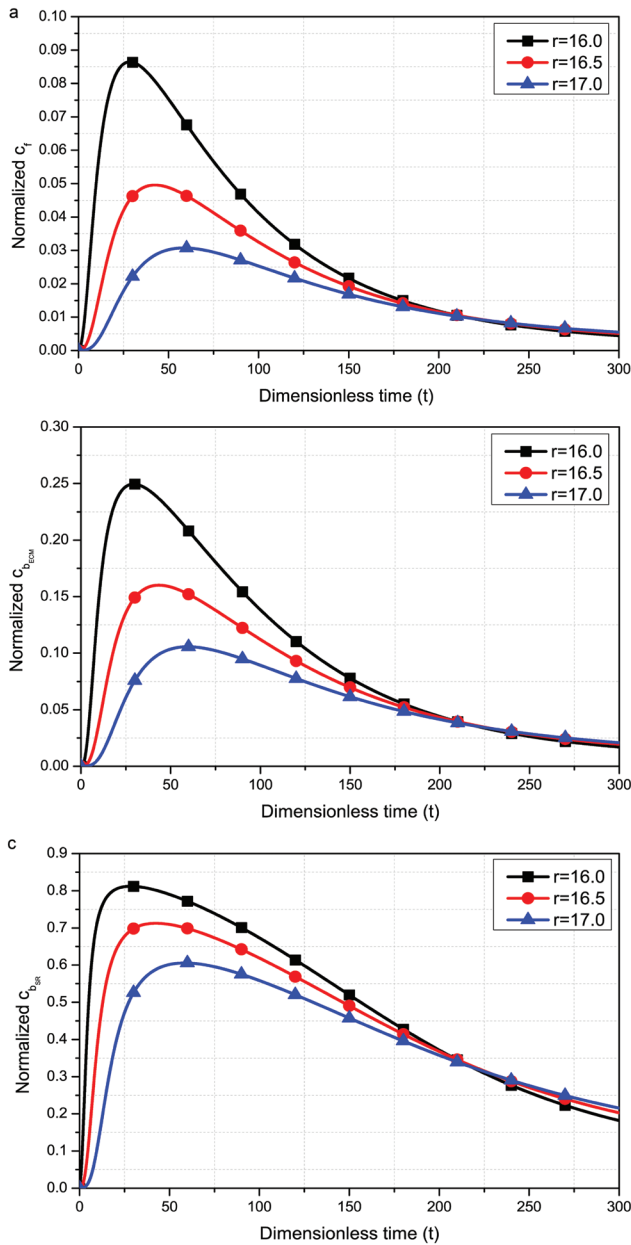


Fig. 4. Drug concentration in the vessel wall versus time for different radial positions at $z = 21.5$. (a) Free drug; (b) ECM-bound drug; (c) SR-bound drug. Other model parameters are set as in Table 2. Abbreviations: ECM, extracellular matrix; SR, specific receptors.

binding on-rate (k_{on}^{SR}). It has been observed that with increasing receptor binding site density and receptor binding on-rate (*i.e.* increase of Da_2/Pe_2), the mean drug (free and ECM-bound) concentrations decrease. But, the mean SR-bound and total drug concentrations increase with increasing receptor binding site density and receptor binding on-rate (*i.e.* increase of Da_2/Pe_2). It was also observed in Figure 7a–d that the effects of Da_2/Pe_2 on SR-bound and total drugs are more sensitive than free and ECM-bound drugs.

The results in Figure 8a–d, respectively, exhibit the influence of scaling parameter α on the normalized mean free drug, mean ECM-bound drug, mean SR-bound drug and mean total drug

concentrations in the arterial tissue over the entire period of time. Evidently, α , depending on c_{becm}^{max} , increases with a decrease in the ECM binding site density (c_{becm}^{max}) (keeping c_s fixed). It is an obvious observation that if the ECM binding site density decreases (*i.e.* the scaling parameter α increases) then all the mean drug (free, ECM-bound, SR-bound and total) concentrations increase.

The results in Figure 9a–d, respectively, exhibit the influence of scaling parameter α_1 on the normalized mean free drug, mean ECM-bound drug, mean SR-bound drug and mean total drug concentrations in the arterial tissue over the entire period of time. Evidently, α_1 , depending on K_d^{ECM} , increases with an increase of the dissociation (backward) rate constant (K_r^{ECM}) in the ECM binding site and also with a decrease in ECM binding on-rate (k_{on}^{ECM}) (keeping c_s fixed). It is an obvious observation that if the ECM binding on-rate decreases and dissociation (backward) rate constant in the ECM binding site increases (*i.e.* the scaling parameter α_1 increases) then the mean drug (free, SR-bound and total) concentrations increase. But, the mean ECM-bound drug concentration decreases with decreasing ECM binding on-rate and increasing dissociation (backward) rate constant in the ECM binding site (*i.e.* increase of scaling parameter α_1).

The results, shown in Figure 10a–d, respectively, project the influence of scaling parameter β on the normalized mean free drug, mean ECM-bound drug, mean SR-bound drug and mean total drug concentrations in the arterial tissue over the entire period of time. Evidently, β , depending on c_{bsr}^{max} , increases with a decrease in the receptor binding site density (c_{bsr}^{max}) (keeping c_s fixed). It is an obvious observation that if the receptor binding site density decreases (*i.e.* the scaling parameter β increases) then all of the mean drug (free, ECM-bound, SR-bound and total) concentrations increase.

The influence of scaling parameter β_1 on the normalized mean free drug, mean ECM-bound drug, mean SR-bound drug and mean total drug concentrations in the arterial tissue are displayed in Figure 11a–d respectively over a stipulated period of time. Evidently, β_1 , depending on K_d^{SR} , increases with an increase in the dissociation (backward) rate constant (K_d^{SR}) in the receptor binding site and also with a decrease in receptor binding on-rate (K_{on}^{SR}) (keeping c_s fixed). It was observed that with decreasing receptor binding on-rate and increasing dissociation (backward) rate constant in the receptor binding site (*i.e.* increase of β_1), the mean drug (free and ECM-bound) concentrations increase. But, the mean SR-bound and total drug concentrations decrease with decreasing receptor binding on-rate and increasing dissociation (backward) rate constant in the receptor binding site (*i.e.* increase of scaling parameter β_1). It was also observed from Figure 11a–d that the effects of scaling parameter β_1 on SR-bound and total drugs are more sensitive than free and ECM-bound drugs.

Finally, in Figure 12a–c, respectively, the displayed spatial distribution of free, ECM-bound and SR-bound drug concentration may again clearly justify the reduction of late lumen loss at the distal part of the arterial tissue, which again validates the findings of Balakrishnan *et al.*²⁹ The spatial patterns for free, ECM-bound and SR-bound drug concentration in Figure 13a–c, respectively, clearly establish our findings further for the zero-concentration interface condition and constant release kinetics. In the Figure 14a–c, respectively, the spatial distribution of free, ECM-bound and SR-bound drug concentration for the zero-flux interface condition and time-dependent release kinetics is displayed.

Conclusions

In the present work, a novel analytical closed-form solution of

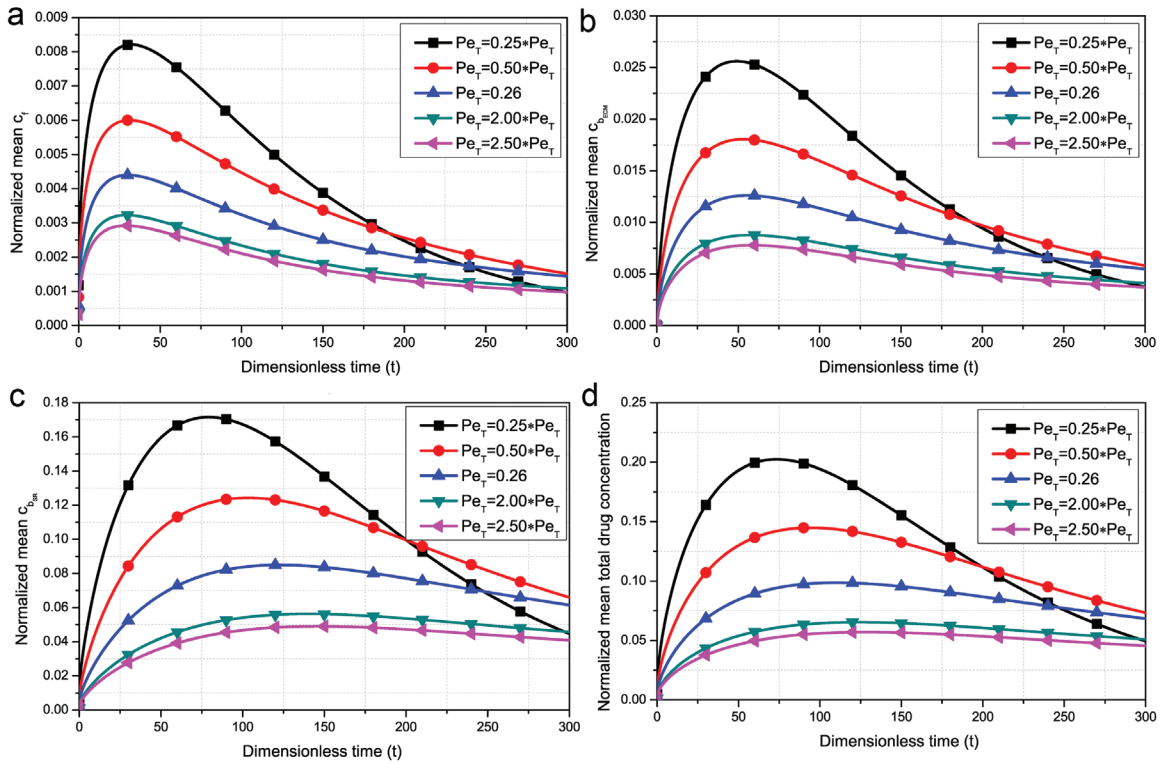


Fig. 5. Mean drug concentration in the vessel wall versus time for different Peclet numbers Pe_T . (a) Free drug; (b) ECM-bound drug; (c) SR-bound drug; (d) Total drug. Other model parameters are set as in Table 2. Abbreviations: ECM, extracellular matrix; SR, specific receptors.

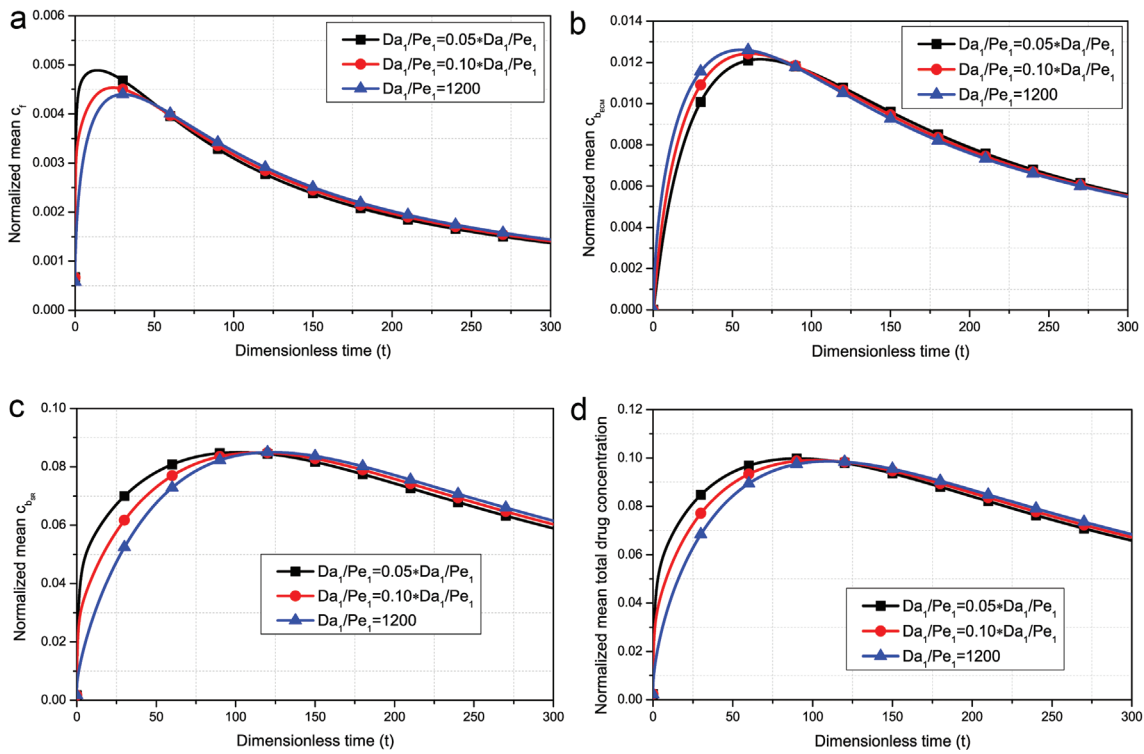


Fig. 6. Mean drug concentration in the vessel wall versus time for different values of Da_1/Pe_1 . (a) Free drug; (b) ECM-bound drug; (c) SR-bound drug; (d) Total drug. Other model parameters are set as in Table 2. Abbreviations: ECM, extracellular matrix; SR, specific receptors.

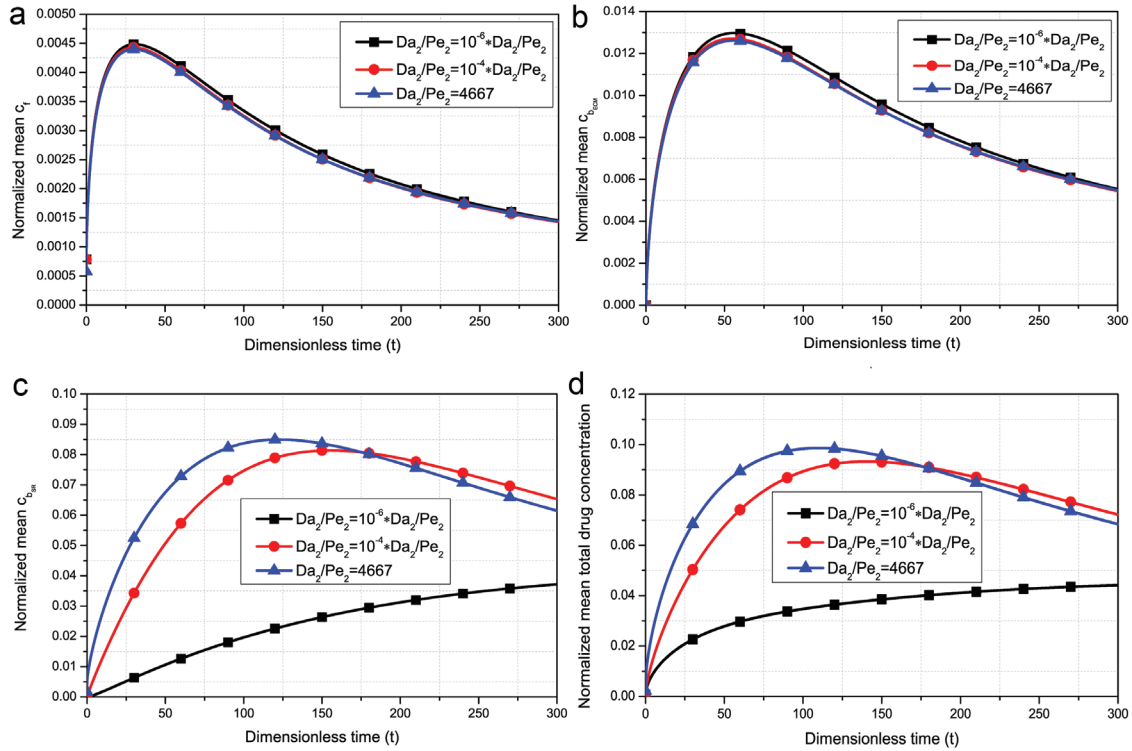


Fig. 7. Mean drug concentration in the vessel wall versus time for different values of Da_2/Pe_2 . (a) Free drug; (b) ECM-bound drug; (c) SR-bound drug; (d) Total drug. Other model parameters are set as in Table 2. Abbreviations: ECM, extracellular matrix; SR, specific receptors.

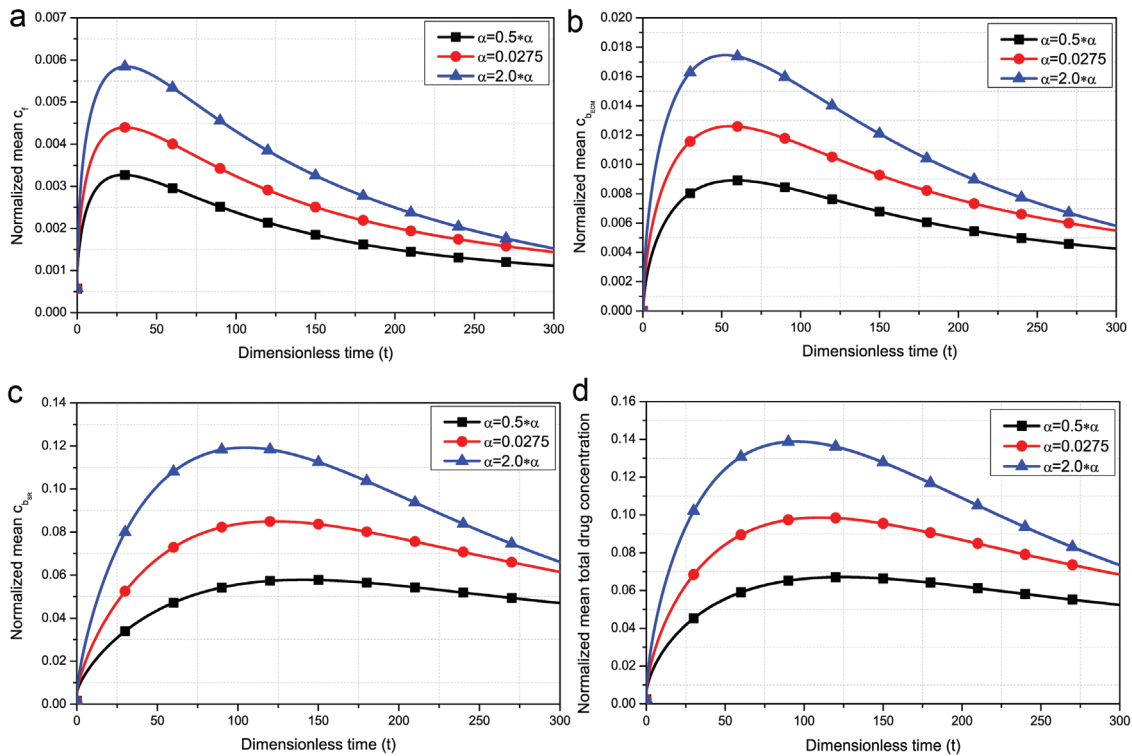


Fig. 8. Mean drug concentration in the vessel wall versus time for different values of the non-dimensional parameter α . (a) Free drug; (b) ECM-bound drug; (c) SR-bound drug; (d) Total drug. Other model parameters are set as in Table 2. Abbreviations: ECM, extracellular matrix; SR, specific receptors.

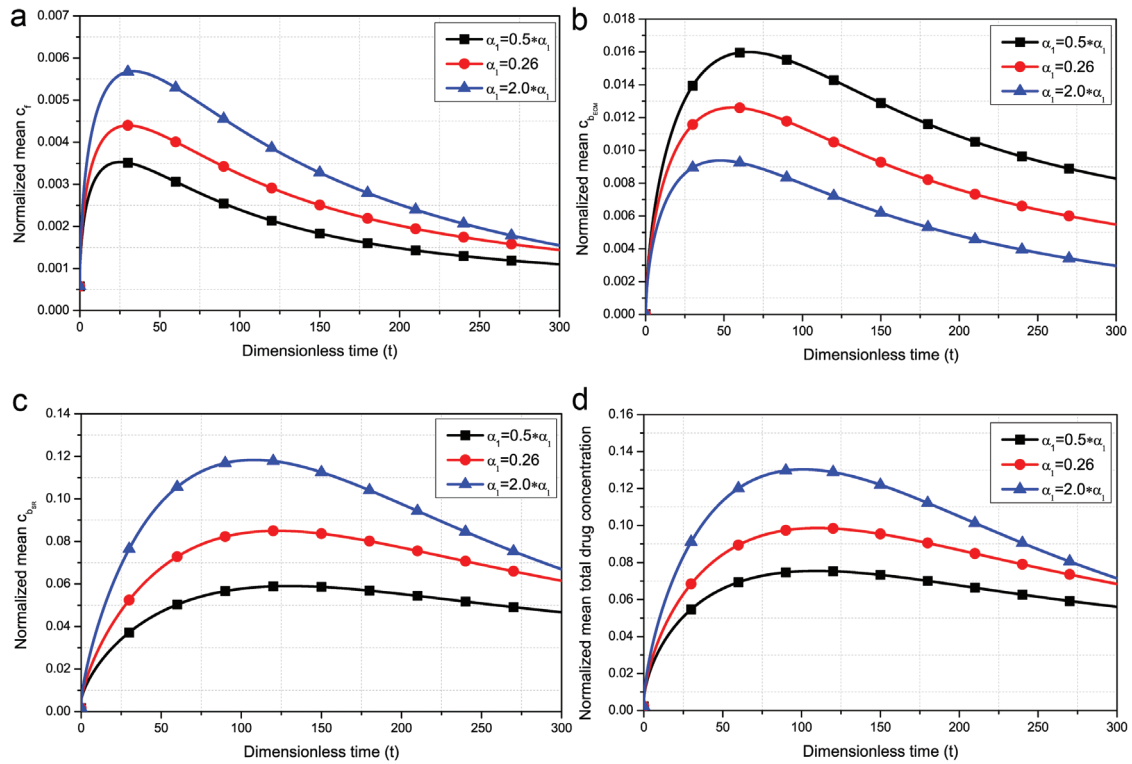


Fig. 9. Mean drug concentration in the vessel wall versus time for different values of the non-dimensional parameter α_1 . (a) Free drug; (b) ECM-bound drug; (c) SR-bound drug; (d) Total drug. Other model parameters are set as in Table 2. Abbreviations: ECM, extracellular matrix; SR, specific receptors.

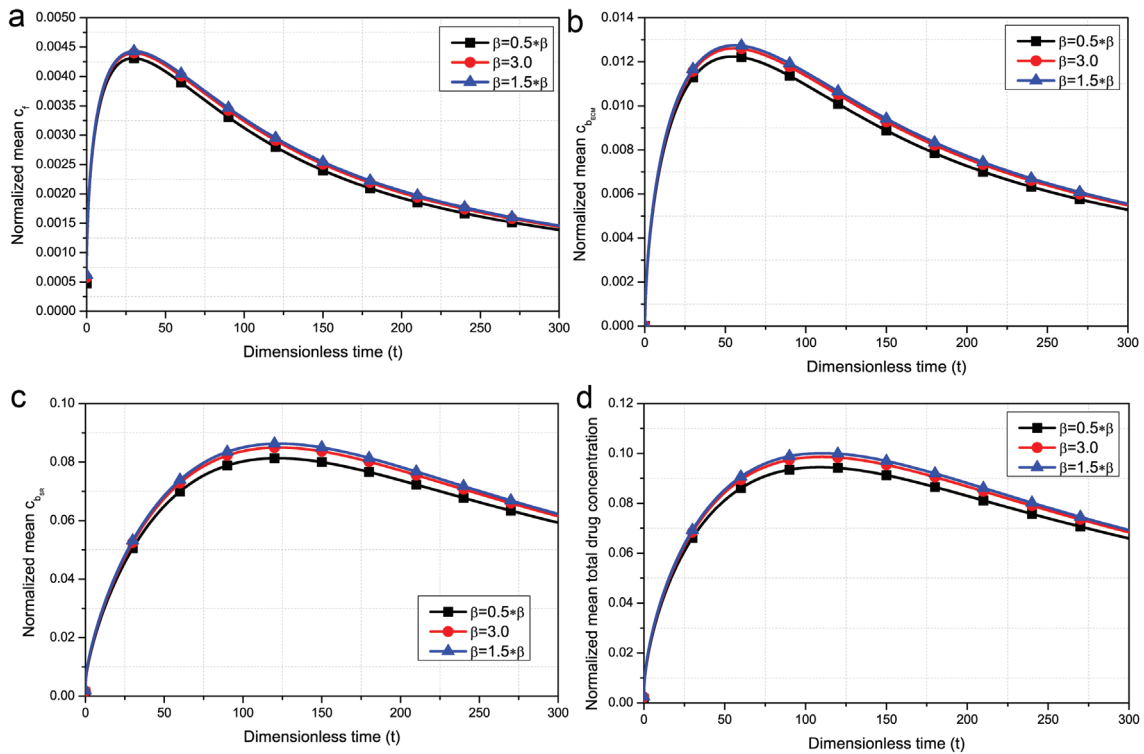


Fig. 10. Mean drug concentration in the vessel wall versus time for different values of the non-dimensional parameter β . (a) Free drug; (b) ECM-bound drug; (c) SR-bound drug; (d) Total drug. Other model parameters are set as in Table 2. Abbreviations: ECM, extracellular matrix; SR, specific receptors.

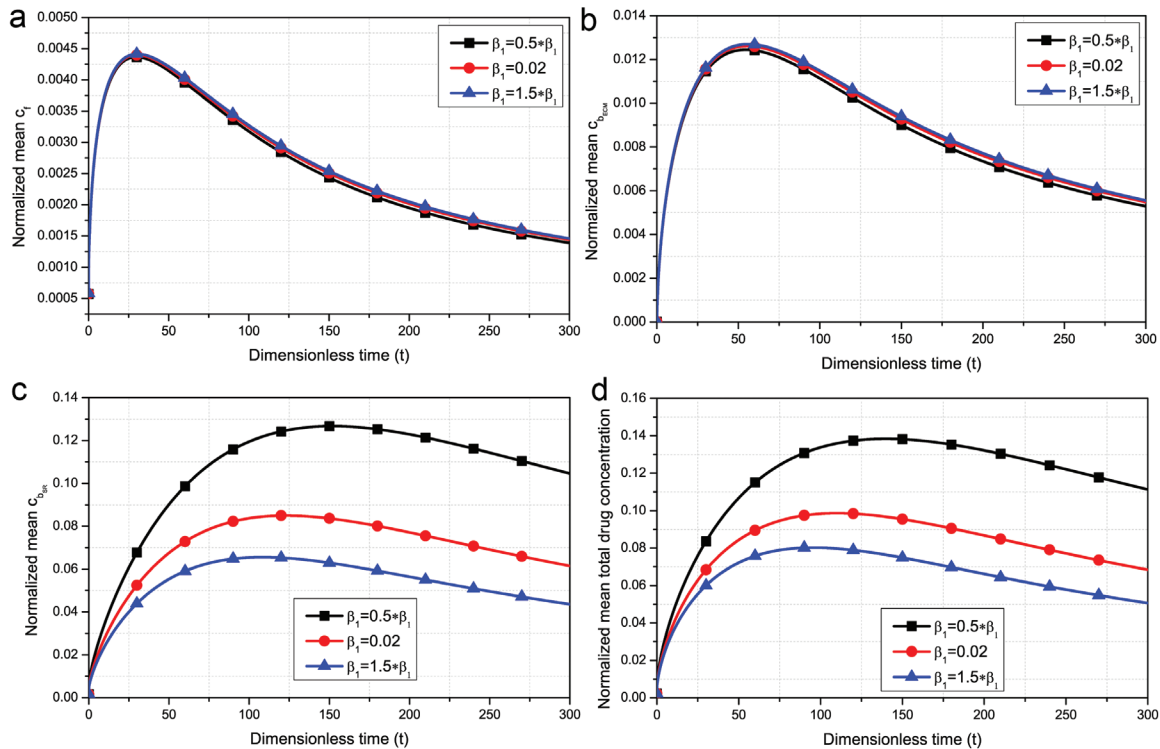


Fig. 11. Mean drug concentration in the vessel wall versus time for different values of the non-dimensional parameter β_1 . (a) Free drug; (b) ECM-bound drug; (c) SR-bound drug; (d) Total drug. Other model parameters are set as in Table 2. Abbreviations: ECM, extracellular matrix; SR, specific receptors.

a 2D axi-symmetric model of drug transport eluted from a coronary DES is proposed and focused on the reversible and saturable binding processes in the vascular tissue. The model is based on a single-layered homogeneous multiple-phase system where a system of partial differential equations describes both the dissolution and diffusion processes in the polymeric layer as well as diffusion, convection and reaction in the tissue. The closed-form solution has been established by using the MAC method.

The salient observations of the above findings are the following:

The penetration length of both free and ECM-bound drug increases with increasing time and saturation of binding sites ultimately takes place.

The SR-bound drug is absorbed at the adventitial boundary with the increase of time.

The drug delivered to the arterial wall from the stent is too low to occupy a large proportion of ECM binding sites, yet is high enough to saturate SR binding sites.

The mean drug (free, ECM-bound, SR-bound and total) concentrations decrease with decreasing porosity and increasing tortuosity of the arterial wall.

With increasing ECM binding site density and ECM binding on-rate, the mean drug (free, SR-bound and total) concentrations decrease. But, the mean ECM-bound drug concentration increases with increasing ECM binding site density and ECM binding on-rate.

Future research directions

Application of this framework to idealized configurations of arteries stented with a DES yielded some general guidelines for future DES design, especially concerning strategies for the effective elu-

tion of the anti-proliferative drug from the stent and its efficacy. Despite these very useful results, many improvements can be envisaged in future models. Limitations of the current model are that the model geometry is 2D axi-symmetric, the considered stent is idealized having three stent struts, and the model is limited to a straight vessel segment. Although the target zone is an atherosclerotic plaque, this consideration has been disregarded here. Inclusion of realistic plaque with anisotropic tissue properties, together with the varying diffusivity of eluted drug within the target lesion, may be the scope of future research.

It will be important to eventually perform the simulations on more realistic three-dimensional geometries where the detailed structure of the stent design is to be taken into account. Based upon the present model validation, the model can be evolved further with the incorporation of several factors, depending on the objectives of the drug release phenomena in various situations, for designing future research in this direction by utilizing the present knowledge of the system.

Medical benefits

Mathematical modelling and numerical simulation are indispensable tools when clinical investigation and/or animal studies are expensive, and in some cases, cumbersome as well. A mathematical model can give us an idea of how an underlying mechanism plays a surrogate role on cardiovascular intervention. The present study gives an overview on the release kinetics and also the binding of sirolimus drug eluted from a coronary stent which helps, certainly, the clinician to estimate the effectiveness of delivery and also the efficacy of drug. Although the present study is an idealized one,

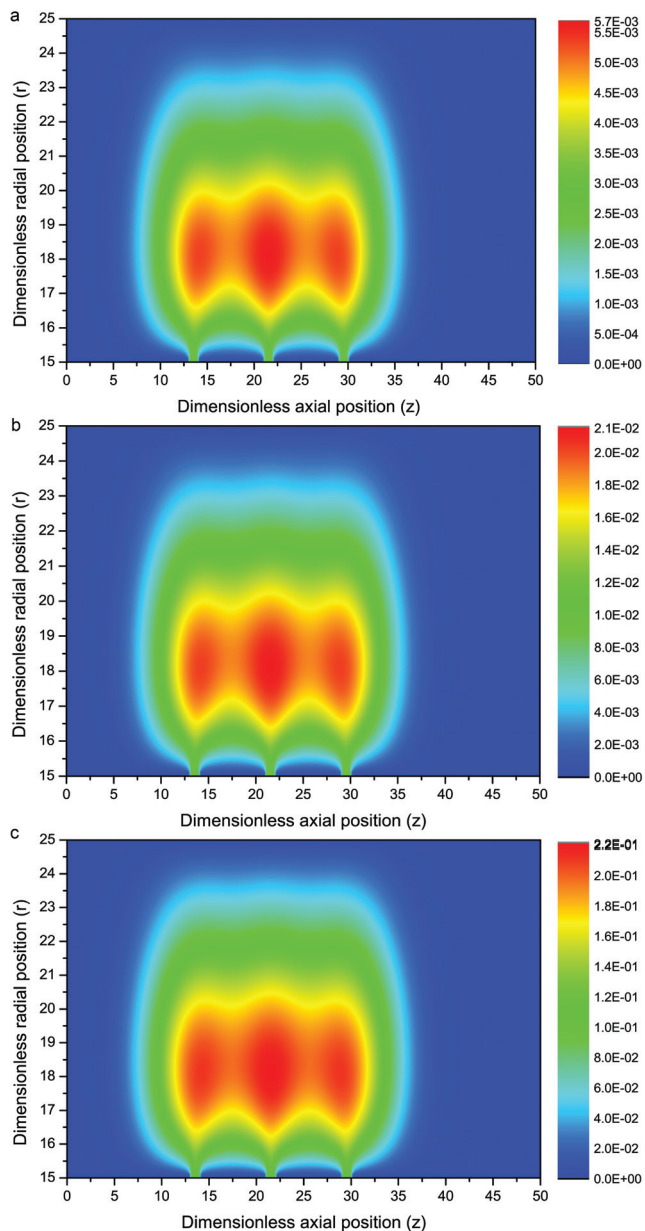


Fig. 12. Visual representation of drug concentration in the vessel wall for time-dependent release kinetics with zero-concentration interface condition in Γ_{bt} at $t = 300$. (a) Free drug; (b) ECM-bound drug; (c) SR-bound drug. Other model parameters are set as in Table 2. Abbreviations: ECM, extracellular matrix; SR, specific receptors.

it will give an idea to the manufacturer in designing next generation of DES. We point out that the results presented here are for the simulated case of sirolimus release and absorption from the Cypher stent.

The significant influence of estimated parameters on the drug masses has been shown graphically, which establishes the strong fact that by altering the parameters, various means of drug release control can be achieved according to the patients' needs. Various conclusions can be drawn from the dynamical behavior of the present model study. It is worth noting that as the drug needs a much longer time in the tissue to get absorbed completely, its effect will

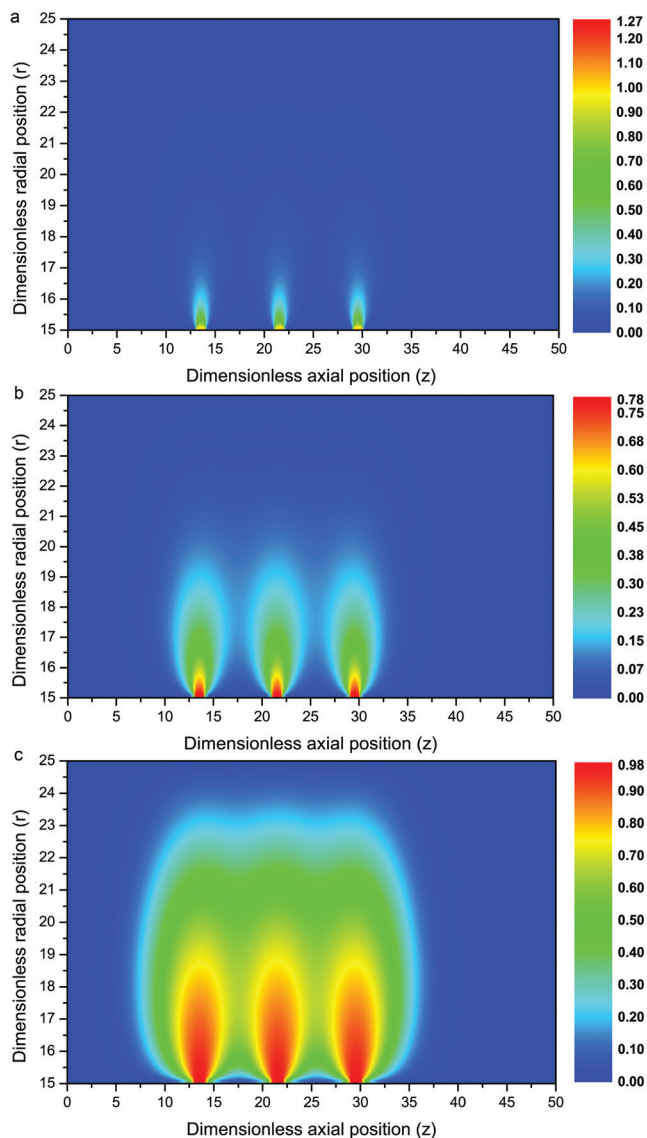


Fig. 13. Visual representation of drug concentration in the vessel wall for constant release kinetics with zero-concentration interface condition in Γ_{bt} at $t = 300$. (a) Free drug; (b) ECM-bound drug; (c) SR-bound drug. Other model parameters are set as in Table 2. Abbreviations: ECM, extracellular matrix; SR, specific receptors.

certainly persist for a long time before the same drug is administered subsequently. This approach may also be applied in any form to other parts of the human body, provided the system does not have major clinical complexity.

Acknowledgments

The author gratefully acknowledges the careful scrutiny and suggestions of the learned reviewers. The author also expresses his gratitude to Professor Prashanta Kumar Mandal, Department of Mathematics, Visva-Bharati University, Santiniketan-731235, West Bengal, India, for fruitful discussions about this paper and for useful support in some numerical tasks.

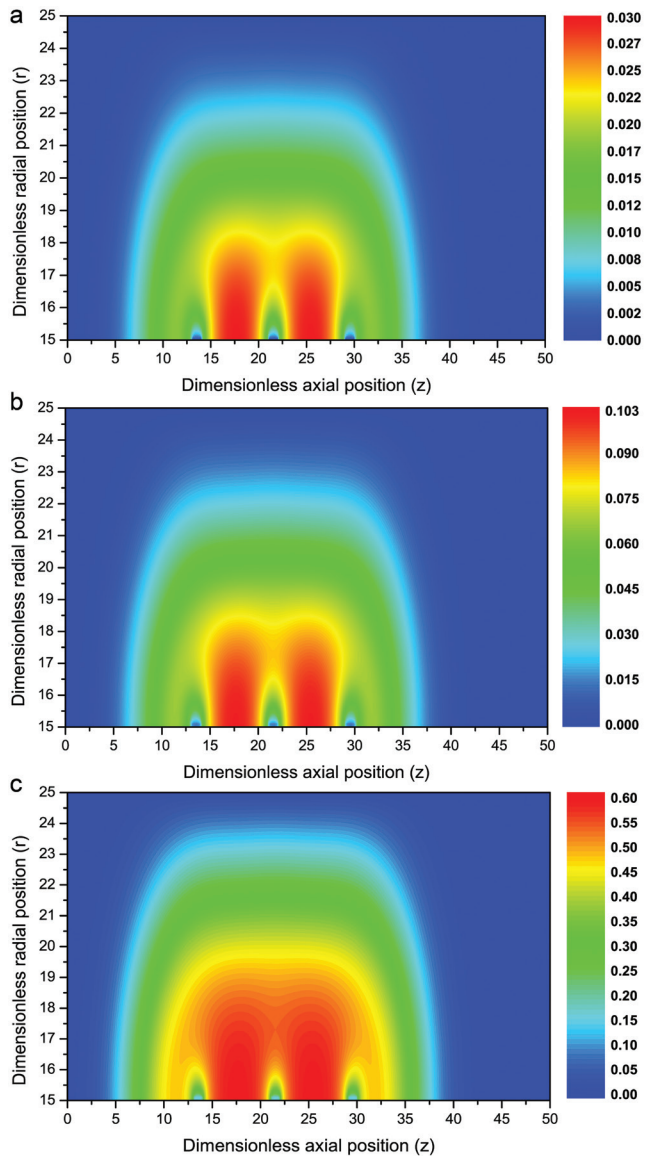


Fig. 14. Visual representation of drug concentration in the vessel wall for time-dependent release kinetics with zero-flux interface condition in r_{bt} at $t = 300$. (a) Free drug; (b) ECM-bound drug; (c) SR-bound drug. Other model parameters are set as in Table 2. Abbreviations: ECM, extracellular matrix; SR, specific receptors.

Conflict of interest

The author declares that no conflict of interest exists.

Author contributions

RS is the sole author.

References

[1] Aragon J, Kar S, Tio F, Trauthen B, Parisky A, Watanabe C, *et al.* The

effect of variable release kinetics on paclitaxel efficacy from a drug eluting stent in a porcine model. *EuroIntervention* 2005;1(2):228–235.

- [2] Guagliumi G, Ikejima H, Sirbu V, Bezerra H, Musumeci G, Lortkipanidze N, *et al.* Impact of drug release kinetics on vascular response to different zotarolimus-eluting stents implanted in patients with long coronary stenoses: the longcot study (optical coherence tomography in long lesions). *JACC Cardiovasc Interv* 2011;4(7):778–785. doi:10.1016/j.jcin.2011.04.007.
- [3] Lovich MA, Philbrook M, Sawyer S, Weselcouch E, Edelman ER. Arterial heparin deposition: role of diffusion, convection, and extravascular space. *Am J Physiol Heart Circ Physiol* 1998;275(6):H2236–H2242. doi:10.1152/ajpheart.1998.275.6.h2236.
- [4] Moses JW, Stone GW, Nikolsky E, Mintz GS, Dangas G, Grube E, *et al.* Drug-eluting stents in the treatment of intermediate lesions: pooled analysis from four randomized trials. *J Am Coll Cardiol* 2006;47(11):2164–2171. doi:10.1016/j.jacc.2006.01.068.
- [5] Serruys PW, Sianos G, Abizaid A, Aoki J, den Heijer P, Bonnier H, *et al.* The effect of variable dose and release kinetics on neointimal hyperplasia using a novel paclitaxel-eluting stent platform: the paclitaxel in-stent controlled elution study (pisces). *J Am Coll Cardiol* 2005;46(2):253–260. doi:10.1016/j.jacc.2005.03.069.
- [6] Migliavacca F, Gervaso F, Prosi M, Zunino P, Minisini S, Formaggia L, *et al.* Expansion and drug elution model of a coronary stent. *Comput Methods Biomech Biomed Engin* 2007;10(1):63–73. doi:10.1080/10255840601071087.
- [7] Borghi A, Foa E, Balossino R, Migliavacca F, Dubini G. Modelling drug elution from stents: effects of reversible binding in the vascular wall and degradable polymeric matrix. *Comput Methods Biomech Biomed Engin* 2008;11(4):367–377. doi:10.1080/10255840801887555.
- [8] Horner M, Joshi S, Dhruva V, Sett S, Stewart S. A two-species drug delivery model is required to predict deposition from drug-eluting stents. *Cardiovasc Eng Technol* 2010;1(3):225–234. doi:10.1007/s13239-010-0016-4.
- [9] Ferreira JA, Naghipoor J, Oliveira Pd. A coupled non-fickian model of a cardiovascular drug delivery system. *Math Med Biol* 2016;33(3):329–357. doi:10.1093/imammb/dqv023.
- [10] Tzafiriri AR, Levin AD, Edelman ER. Diffusion-limited binding explains binary dose response for local arterial and tumour drug delivery. *Cell Proliferation* 2009;42(3):348–363. doi:10.1111/j.1365-2184.2009.00602.x.
- [11] Bozsak F, Chomaz JM, Barakat AI. Modeling the transport of drugs eluted from stents: physical phenomena driving drug distribution in the arterial wall. *Biomech Model Mechanobiol* 2014;13(2):327–347. doi:10.1007/s10237-013-0546-4.
- [12] Bozsak F, Gonzalez-Rodriguez D, Sternberger Z, Belitz P, Bewley T, Chomaz JM, *et al.* Optimization of drug delivery by drug-eluting stents. *PLoS one* 2015;10(6):e0130182. doi:10.1371/journal.pone.0130182.
- [13] Lauffenburger DA, Linderman J. Receptors: models for binding, trafficking, and signaling, Oxford University Press, 1993.
- [14] Tzafiriri AR, Groothuis A, Price GS, Edelman ER. Stent elution rate determines drug deposition and receptor-mediated effects. *J Control Release* 2012;161(3):918–926. doi:10.1016/j.jconrel.2012.05.039.
- [15] McGinty S, Pontrelli G. On the role of specific drug binding in modelling arterial eluting stents. *J Math Chem* 2016;54(4):967–976. doi:10.1007/s10910-016-0618-7.
- [16] McGinty S, Pontrelli G. A general model of coupled drug release and tissue absorption for drug delivery devices. *J Control Release* 2015;217:327–336. doi:10.1016/j.jconrel.2015.09.025.
- [17] O'Connell BM, Walsh MT. Demonstrating the influence of compression on artery wall mass transport. *Ann Biomed Eng* 2010;38(4):1354–1366. doi:10.1007/s10439-010-9914-8.
- [18] Balakrishnan B, Dooley JF, Kopia G, Edelman ER. Intravascular drug release kinetics dictate arterial drug deposition, retention, and distribution. *J Control Release* 2007;123(2):100–108. doi:10.1016/j.jconrel.2007.06.025.
- [19] Balakrishnan B, Dooley J, Kopia G, Edelman ER. Thrombus causes fluctuations in arterial drug delivery from intravascular stents. *J Control Release* 2008;131(3):173–180. doi:10.1016/j.jconrel.2008.07.027.
- [20] Hwang CW, Wu D, Edelman ER. Physiological transport forces

- govern drug distribution for stent-based delivery. *Circulation* 2001;104(5):600–605. doi:10.1161/hc3101.092214.
- [21] Levin AD, Jonas M, Hwang CW, Edelman ER. Local and systemic drug competition in drug-eluting stent tissue deposition properties. *J Control Release* 2005;109(1):236–243. doi:10.1016/j.jconrel.2005.09.041.
- [22] Bierer BE, Mattila PS, Standaert RF, Herzenberg LA, Burakoff SJ, Crabtree G, *et al.* Two distinct signal transmission pathways in T lymphocytes are inhibited by complexes formed between an immunophilin and either fk506 or rapamycin. *Proceedings of the National Academy of Sciences* 1990;87(23):9231–9235. doi:10.1073/pnas.87.23.9231.
- [23] Kolachalama VB, Levine EG, Edelman ER. Luminal flow amplifies stent-based drug deposition in arterial bifurcations. *PLoS one* 2009;4(12):e8105. doi:10.1371/journal.pone.0008105.
- [24] Kolandaivelu K, O'Brien CC, Shazly T, Edelman ER, Kolachalama VB. Enhancing physiologic simulations using supervised learning on coarse mesh solutions. 2015;12(104):20141,073. doi:10.1098/rsif.2014.1073.
- [25] Higuchi T. Mechanism of sustained-action medication. theoretical analysis of rate of release of solid drugs dispersed in solid matrices. *J Pharm Sci* 1963;52(12):1145–1149. doi:10.1002/jps.2600521210.
- [26] O'Brien CC, Kolachalama VB, Barber TJ, Simmons A, Edelman ER. Impact of flow pulsatility on arterial drug distribution in stent-based therapy. *J Control Release* 2013;168(2):115–124. doi:10.1016/j.jconrel.2013.03.014.
- [27] Kolachalama VB, Pacetti SD, Franses JW, Stankus JJ, Zhao HQ, Shazly T, *et al.* Mechanisms of tissue uptake and retention in zotarolimus-coated balloon therapy. *Circulation* 2013;127(20):2047–2055. doi:10.1161/circulationaha.113.002051.
- [28] Saha R, Mandal PK. Modelling time-dependent release kinetics in stent-based delivery. *J Explor Res Pharmacol* 2018;3:61–70. doi:10.14218/JERP.2018.00001.
- [29] Balakrishnan B, Tzafiriri AR, Seifert P, Groothuis A, Rogers C, Edelman ER. Strut position, blood flow, and drug deposition implications for single and overlapping drug-eluting stents. *Circulation* 2005;111(22):2958–2965. doi:10.1161/circulationaha.104.512475.
- [30] Ferdous J, Chong C. Effect of atherosclerotic plaque on drug delivery from drug-eluting stent. 13th International Conference on Biomedical Engineering, Springer, 2009, pp. 1519–1522. doi:10.1007/978-3-540-92841-6_376.
- [31] Huang Z, Tarbell J. Numerical simulation of mass transfer in porous media of blood vessel walls. *Am J Physiol* 1997;273(1 Pt 2):H464–H477. doi:10.1152/ajpheart.1997.273.1.h464.
- [32] Levin AD, Vukmirovic N, Hwang CW, Edelman ER. Specific binding to intracellular proteins determines arterial transport properties for rapamycin and paclitaxel. *Proc Natl Acad Sci U S A* 2004;101(25):9463–9467. doi:10.1073/pnas.0400918101.
- [33] McGinty S. Stents and arterial flows. PhD thesis, University of Strathclyde, 2010.
- [34] McGinty S, McKee S, Wadsworth RM, McCormick C. Modelling drug-eluting stents. *Math Med Biol* 2011;28(1):1–29. doi:10.1093/imamb/dqq003.
- [35] Sakharov DV, Kalachev LV, Rijken DC. Numerical simulation of local pharmacokinetics of a drug after intravascular delivery with an eluting stent. *J Drug Target* 2002;10(6):507–513. doi:10.1080/1061186021000038382.
- [36] Tedgui A, Lever M. Filtration through damaged and undamaged rabbit thoracic aorta. *Am J Physiol Heart Circ Physiol* 1984;247(5):H784–H791. doi:10.1152/ajpheart.1984.247.5.h784.
- [37] Vairo G, Cioffi M, Cottone R, Dubini G, Migliavacca F. Drug release from coronary eluting stents: a multidomain approach. *J Biomech* 2010;43(8):1580–1589. doi:10.1016/j.jbiomech.2010.01.033.
- [38] Wear MA, Walkinshaw MD. Determination of the rate constants for the fk506 binding protein/rapamycin interaction using surface plasmon resonance: An alternative sensor surface for Ni²⁺-nitrilotriacetic acid immobilization of His-tagged proteins. *Anal Biochem* 2007;371(2):250–252. doi:10.1016/j.ab.2007.06.034.
- [39] Zunino P. Multidimensional pharmacokinetic models applied to the design of drug-eluting stents. *Cardiovascular Engineering: An International Journal* 2004;4(2):181–191. doi:10.1023/b:care.0000031547.39178.cb.